University of Birmingham

A power electronic traction transformer for a medium voltage DC electric railway system

Ferencz, Izsak; Petreus, Dorin; Tricoli, Pietro

Document Version
Peer reviewed version

Citation for published version (Harvard):
Ferencz, I, Petreus, D & Tricoli, P 2021, A power electronic traction transformer for a medium voltage DC electric railway system. in *Proceedings: 2021 44th International Spring Seminar on Electronics Technology (ISSE).*, 9467646, International Spring Seminar on Electronics Technology, Institute of Electrical and Electronics Engineers (IEEE), 2021 44th International Spring Seminar on Electronics Technology (ISSE), Dresden , Germany, 5/05/21. https://doi.org/10.1109/ISSE51996.2021.9467646

[Link to publication on Research at Birmingham portal](#)

A Power Electronic Traction Transformer for
a Medium Voltage DC Electric Railway System

Izsák Ferencz[1], Dorin Petreuş[1], and Pietro Tricoli [2]

[1] Department of Applied Electronics, Technical University of Cluj-Napoca, Romania
[2] Department of Electronic, Electrical and Systems Engineering, University of Birmingham, United Kingdom
izsak.ferencz@ael.utcluj.ro

Abstract*: Power Electronic Traction Transformers (PETT) are a trend in railway traction because of higher power density and efficiency. A PETT system achieves this by having Medium Frequency Transformers (MFT) in their converter modules as galvanic isolation. The latest PETT systems use Wide Band Gap (WBG) semiconductors to further increase system efficiency. All state of the art PETT systems are developed for the Medium Voltage (MV) AC Railway Electrification Systems (RES). This work however, proposes a PETT system for a novel MV DC RES. In another article, we already studied, evaluated and presented different state of the art PETT topologies to choose an optimal one for this application. The paper will present simulation results for an 8-module Input Series Output Parallel (ISOP) MVDC PETT system capable of 1.2MW of total power. The converter topology used in the modules is Dual Active Bridge (DAB). In this paper, a decoupling method is also deduced for 8 modules to control each module separately. Results show how modules with different initial capacitor voltage are self-balancing and stabilizing at the same input voltage value. The results and theoretical notions obtained in this project will lay the foundation of a novel smart MVDC RES.*

1. INTRODUCTION

The goal of this project is to present a novel RES, which is a smart interoperable MVDC railway grid, compatible with renewable energy plants. In the past, technology not being advanced enough MVDC railway electrification was not possible to be implemented, therefore MVAC railway electrification became the most popular and in some areas LVDC systems [1]. In [2], our previous article it was already compared in detail the MVDC and MVAC RES. The new MVDC RES combines the advantage of a DC system with the advantages of using medium-voltage. Also in [2], after an overview of state of the art topologies, the modular ISOP structure is chosen with a DAB converter.

In this paper, the Simulink model and simulations of a whole MVDC catenary-line fed PETT system will be presented with a decoupled voltage loop control system. In [3], Mohan demonstrates that in an ISOP system, the same control loop applied for all modules will achieve stability, therefore as a first step in our work was to implement the system with a single control loop. After successful simulation however,

based on [4] the system was further developed. In [4] it is stated, that due to input voltage or inductance mismatch in modules, one control loop for all modules may not reach a well-balanced input stage and the article presents a decoupling method for a 3 modules system in ISOP connection. In our paper, the detailed calculations and formulas are deduced for an ISOP system with 8 modules and then applied on our PETT system successfully, with separate compensator loop for each module. A traction drive and motor is also attached to the PETT, however not treated here.

Section 2 presents the mathematical model of the DAB converter, then section 3 contains the mathematical deductions of the decoupling control strategy. In section 4 the simulation model and results are discussed. Finally section 5 draws the conclusions.

2. DAB CONVERTER – MATHEMATICAL MODEL

The mathematical model of a DAB converter can be deduced starting from its waveforms. For this purpose the voltage and current waveforms of the leakage inductor is analyzed in detail to develop the average model [5].
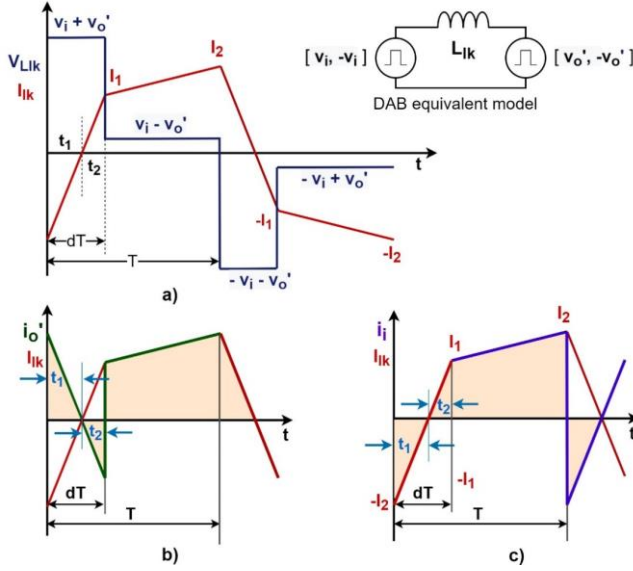
Fig. 1. DAB converter - waveforms: a) presents the leakage inductor voltage and current, b) shows the output current reflected in the primary, compared to the leakage inductor current i_L and c) represents the input current compared to i_L.

As seen on Fig. 1a), for the interval $0 < t < d \cdot T$, the voltage on the leakage inductor is the sum of the input voltage – noted v_i, and the output voltage reflected in the primary – noted v_o' ($v_o' = v_o/n$, where n is the transformer turn ratio). Similarly, for the interval $d \cdot T < t < T$ the inductor voltage is then v_i - v_o', d being the time delay. Therefore, the inductor voltage has the following equation as a function of the value of the inductor – L_{lk}, the half of the switching period – T, and the peak values of the inductor current – I_1 and I_2:

$$V_{lk} = \begin{cases} v_i + v'_o = L_{lk} \dfrac{I_1 + I_2}{d \cdot T}, & for \ 0 < t < d \cdot T \\ v_i - v'_o = L_{lk} \dfrac{I_2 - I_1}{(1 - d) \cdot T}, & for \ d \cdot T < t < T \end{cases} \quad (1)$$

Adding the two equations and then subtracting them one can obtain the value of I_2 and I_1, the two peaks:

$$\begin{cases} I_1 = \dfrac{T}{2L_{lk}}(2dv_i + v'_o - v_i) \\ I_2 = \dfrac{T}{2L_{lk}}(2dv'_o + v_i - v'_o) \end{cases} \quad (2)$$

Then looking at Fig. 1.b) and 1.c), $d \cdot T$ is split in two subintervals, t_1 and t_2 with the following conditions:

$$\begin{cases} t_1 + t_2 = d \cdot T \\ \dfrac{I_2}{t_1} = \dfrac{I_1}{t_2} \end{cases} \quad (3)$$

From (3) t_1 and t_2 is obtained, if we divide I_2 with I_1 from (2) and then I_1 with I_2:

$$\begin{cases} t_1 = T\dfrac{2dv'_o + v_i - v'_o}{2(v'_o + v_i)} \\ t_2 = T\dfrac{2dv_i + v'_o - v_i}{2(v'_o + v_i)} \end{cases} \quad (4)$$

Having the peak values I_1 and I_2 and the time intervals t_1 and t_2 for the leakage inductor current, the average input and output current can be calculated, using Fig. 1.b) and 1.c):

$$\begin{cases} i_{i_{avg}} = \dfrac{1}{T}\left[-\dfrac{1}{2}I_2t_1 + \dfrac{1}{2}I_1t_2 + (1-d)T\dfrac{1}{2}(I_1 + I_2)\right] \\ i_{o'_{avg}} = \dfrac{1}{T}\left[\dfrac{1}{2}I_2t_1 - \dfrac{1}{2}I_1t_2 + (1-d)T\dfrac{1}{2}(I_1 + I_2)\right] \end{cases} \quad (5)$$

2.1. Average model

The average model now can be obtained from (2), (4) and (5), rewriting the average currents as [5]:

$$\begin{cases} i_{i_{avg}} = \dfrac{(1-d)dTv_o}{nL_{lk}} \\ i_{o'_{avg}} = \dfrac{(1-d)dTv_i}{L_{lk}} \end{cases} \quad (6)$$

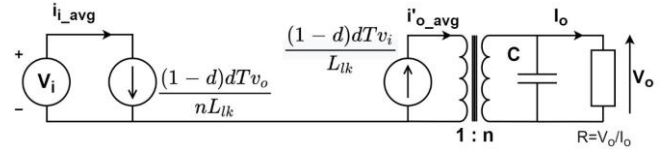Based on (6), the average model looks like in Fig. 2:

Fig. 2. DAB converter average model.

Using this model, the output voltage is expressed as a function of the input voltage and the load, as follows:

$$v_o = \frac{d(1-d)TRv_i}{nL_{lk}} \quad (7)$$

The transferred power is:

$$P_o = \frac{d(1-d)Tv_iv_o}{nL_{lk}} \quad (8)$$

Finally, from (7) the voltage transfer ratio as a function of the phase-shift between the primary and secondary bridges is obtained [6]:

$$M = \frac{v_o}{nv_i} = \frac{d(1-d)TR}{n^2L_{lk}} = d(1-d)k \quad (9)$$

3. DECOUPLED CONTROL STRATEGY OF THE MULTI-MODULAR ISOP CONNECTED PETT

Connecting power converters in ISOP configuration is a popular method to achieve higher

power transfer and power density. Using the same converters in each module simplifies their interconnection, however input voltage balance problems can appear due to imperfections, parasitic and other errors, even if they have the same constructive values, possibly leading to a voltage, current and inductance mismatch. This means, that if the same control system operates each module, these mismatches will not be balanced. However, the equations of the system shows that the electrical quantities of the converters and the control signals are interdependent, also, the voltage distribution depends on parasitic components. This can produce uncertainty of the input voltage distribution. To present this problem and its solution a PETT with 8 DAB modules is considered, as in Fig. 4. The converter bridges are operated with fixed duty cycle of 50% and the control variable is the phase shift between the primary and secondary side bridges. The proposed solution is the decoupling of control variables to obtain separate control loop for each module in a way that ZVS capability to be maintained [4].
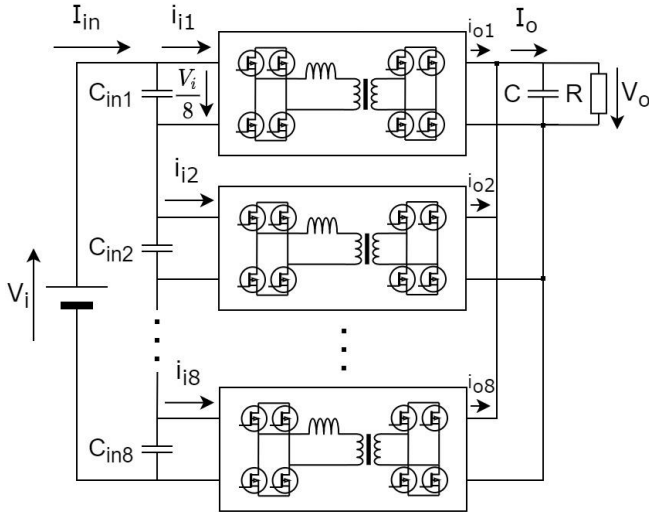

Fig. 4. Eight modules DAB converter in ISOP connection.

Modelling the converters in ISOP connection, each bridge can be considered a dependent current source. The equations of the average input and output currents has to be perturbed to obtain the model equations:

$$\begin{cases} \hat{\imath}_{oj} = \left.\dfrac{\partial i_{o_{avg}}}{\partial d}\right|_0 \hat{d} + \left.\dfrac{\partial i_{o_{avg}}}{\partial v_i}\right|_0 \widehat{v_i} = g_{od} \cdot \hat{d} + g_{ov_i} \cdot \widehat{v_i} \\ \hat{\imath}_{ij} = \left.\dfrac{\partial i_{i_{avg}}}{\partial d}\right|_0 \hat{d} + \left.\dfrac{\partial i_{i_{avg}}}{\partial v_o}\right|_0 \widehat{v_o} = g_{id} \cdot \hat{d} + g_{iv_o} \cdot \widehat{v_o} \end{cases} \quad (10)$$

Where j is the module number and the coefficients g_{od}, g_{id}, g_{ovi} and g_{ivo} are:

$$\begin{cases} g_{od} = \dfrac{v_i T(1-2d)}{nL_{lk}} = \dfrac{v_o(1-2d)}{(1-d)dR} \\ g_{id} = \dfrac{v_o T(1-2d)}{nL_{lk}} = \dfrac{v_o^2(1-2d)}{v_i(1-d)dR} = \dfrac{v_o}{v_i}g_{od} \\ g_{ovi} = g_{ivo} = \dfrac{Td(1-d)}{nL_{lk}} = \dfrac{v_o}{v_i R} \end{cases} \quad (11)$$

In this model in Fig. 4 it is assumed that all the modules have the same component values (leakage inductance, transformer turn ration, switching period and input capacitors), input voltage ($v_i=V_i/8$) and time-shift of bridge control signals (d). Although the perturbations are different for each ($\widehat{d_1} \neq \widehat{d_2} \neq \cdots \neq \widehat{d_8}$). Based on (10) $\widehat{v_o}$ for the 8 module system is:

$$\widehat{v_o} = \frac{R}{RCs+1} \cdot \begin{bmatrix} g_{od} \cdot (\widehat{d_1} + \widehat{d_2} + \cdots + \widehat{d_8}) + \\ +g_{ovi} \cdot (\widehat{v_{i1}} + \widehat{v_{i2}} + \cdots + \widehat{v_{i8}}) \end{bmatrix} \quad (12)$$

If we consider the total input voltage constant, then the sum of input voltages will be zero, since it is equal to the total input voltage. Thus, the equation will simplify as:

$$\widehat{v_o} = \frac{R}{RCs+1} \cdot g_{od} \cdot (\widehat{d_1} + \widehat{d_2} + \cdots + \widehat{d_8}) = \\ = G_{vd} \cdot (\widehat{d_1} + \widehat{d_2} + \cdots + \widehat{d_8}) \quad (13)$$

From the input port of each module the total input current can be obtained:

$$\begin{cases} \hat{\imath}_i = \widehat{\imath_{i1}} + \widehat{v_{i1}} \cdot C_i s \\ \hat{\imath}_i = \widehat{\imath_{i2}} + \widehat{v_{i2}} \cdot C_i s \\ \quad\vdots \\ \hat{\imath}_i = \widehat{\imath_{i8}} + \widehat{v_{i8}} \cdot C_i s \end{cases} \quad (14)$$

Adding the equations in (14) the expression of the total input current is found:

$$\hat{\imath}_i = \frac{1}{8}(\widehat{\imath_{i1}} + \widehat{\imath_{i2}} + \cdots + \widehat{\imath_{i8}}) + \\ + \frac{1}{8}(\widehat{v_{i1}} + \widehat{v_{i2}} + \cdots + \widehat{v_{i8}}) \cdot C_i s \quad (15)$$

Considering the total input voltage to be constant, based on (10), $\hat{\imath}_i$ is:

$$\hat{\imath}_i = \frac{1}{8} \cdot \left[g_{id} \cdot (\widehat{d_1} + \widehat{d_2} + \cdots + \widehat{d_8}) + 8 \cdot g_{ivo} \cdot \widehat{v_o} \right] \quad (16)$$

Substituting (13) into (16), $\hat{\imath}_i$ finally is:

$$\hat{\imath}_i = (\widehat{d_1} + \widehat{d_2} + \cdots + \widehat{d_8}) \cdot \left(\frac{1}{8} \cdot g_{id} + g_{ivo} \cdot G_{vd} \right) = \\ = G_{ind} \cdot (\widehat{d_1} + \widehat{d_2} + \cdots + \widehat{d_8}) \quad (17)$$

Then from (17), the input voltage for the first module is:

$$\begin{cases} \widehat{v_{\iota 1}} = \dfrac{\widehat{\iota_i} - \widehat{\iota_{\iota 1}}}{C_i s} \\ \widehat{v_{\iota 1}} = \dfrac{1}{C_i s} \cdot \begin{bmatrix} G_{ind} \cdot (\widehat{d_1} + \widehat{d_2} + \cdots + \widehat{d_8}) - \\ -(g_{id} \cdot \widehat{d_1} + g_{ivo} \cdot \widehat{v_o}) \end{bmatrix} \end{cases} \quad (18)$$

Substituting (13) into (18) and then using G_{ind} from (17), the input voltage can be finally developed as:

$$\widehat{v_{\iota 1}} = \frac{1}{C_i s} \cdot \left[\frac{1}{8} \cdot g_{id} \cdot (\widehat{d_1} + \widehat{d_2} + \cdots + \widehat{d_8}) - g_{id} \cdot \widehat{d_1} \right] \quad (19)$$

The control strategy chosen for decoupling the variables is N-1 (where N is the number of modules, 8) input voltages controlled by separate control loops and another loop for the output voltage. To summarize the ISOP model equations the variable $A(s)$ is defined:

$$A(s) = \frac{g_{id}}{8C_i s} = \frac{1}{8C_i s} \frac{T}{L_{lk} \cdot n} V_o (1 - 2d) \quad (20)$$

Then based on (20) the input voltages of the first three modules are:

$$\begin{cases} \widehat{v_{\iota 1}} = A(s) \cdot (\widehat{d_2} + \cdots + \widehat{d_8} - 7 \cdot \widehat{d_1}) \\ \quad\quad \vdots \\ \widehat{v_{\iota 7}} = A(s) \cdot (\widehat{d_1} + \cdots + \widehat{d_6} + \widehat{d_8} - 7 \cdot \widehat{d_7}) \end{cases} \quad (21)$$

Finally, using (21) and (13), the matricidal form of the model equations can be written:

$$\begin{bmatrix} \widehat{v_{\iota 1}} \\ \vdots \\ \widehat{v_{\iota 7}} \\ \widehat{v_o} \end{bmatrix} = \begin{bmatrix} -7A(s) & \cdots & A(s) & A(s) \\ \vdots & \ddots & \vdots & \vdots \\ A(s) & \cdots & -7A(s) & A(s) \\ G_{vd}(s) & \cdots & G_{vd}(s) & G_{vd}(s) \end{bmatrix} \cdot \begin{bmatrix} \widehat{d_1} \\ \widehat{d_2} \\ \vdots \\ \widehat{d_8} \end{bmatrix} =$$

$$= H(s) \cdot \begin{bmatrix} \widehat{d_1} \\ \widehat{d_2} \\ \vdots \\ \widehat{d_8} \end{bmatrix} \quad (22)$$

In (22) can be noticed that the variation of normalized time-shifts $\widehat{d_j}$ affects all the controlled quantities forming a MIMO (multiple input, multiple output) system from the modular converter, in which the quantities and signals are interdependent. The system must be manipulated to consider each module a SISO (single input, single output) system [4][7]. This can be achieved by applying the aforementioned control strategy. If the H(s) 8x8 matrix in (22) would be diagonal, each control signal would control a single quantity and each control quantity will depend on one signal only. Therefore, H(s) has to be decomposed into a diagonal matrix D(s) and a transition matrix Y(s) and then the inverse matrix of Y(s) must be calculated to obtain how the new set of control variables interacts with the original ones.

$$H(s) = D(s) \cdot Y(s) = \begin{bmatrix} 8A(s) & 0 & \cdots & 0 \\ 0 & 8A(s) & \cdots & 0 \\ \vdots & \vdots & \ddots & \vdots \\ 0 & 0 & \cdots & 8G_{vd}(s) \end{bmatrix} \cdot Y(s) \quad (23)$$

Now the product of Y(s) and the control variables will form a new set of control variables.

$$\begin{bmatrix} \widehat{v_{\iota 1}} \\ \vdots \\ \widehat{v_{\iota 7}} \\ \widehat{v_o} \end{bmatrix} = \begin{bmatrix} 8A(s) & 0 & \cdots & 0 \\ 0 & 8A(s) & \cdots & 0 \\ \vdots & \vdots & \ddots & \vdots \\ 0 & 0 & \cdots & 8G_{vd}(s) \end{bmatrix} \cdot \begin{bmatrix} \widehat{x_1} \\ \widehat{x_2} \\ \vdots \\ \widehat{x_8} \end{bmatrix} \quad (24)$$

$$Y(s) = D(s)^{-1} \cdot H(s) = \begin{bmatrix} \dfrac{1}{8A(s)} & 0 & 0 & 0 \\ 0 & \dfrac{1}{8A(s)} & 0 & 0 \\ 0 & 0 & \dfrac{1}{8A(s)} & 0 \\ 0 & 0 & 0 & \dfrac{1}{8G_{vd}(s)} \end{bmatrix} \cdot$$

$$\cdot \begin{bmatrix} -7A(s) & \cdots & A(s) & A(s) \\ \vdots & \ddots & \vdots & \vdots \\ A(s) & \cdots & -7A(s) & A(s) \\ G_{vd}(s) & \cdots & G_{vd}(s) & G_{vd}(s) \end{bmatrix} = \begin{bmatrix} -\frac{7}{8} & \frac{1}{8} & \frac{1}{8} & \frac{1}{8} \\ \frac{1}{8} & -\frac{7}{8} & \frac{1}{8} & \frac{1}{8} \\ \frac{1}{8} & \frac{1}{8} & -\frac{7}{8} & \frac{1}{8} \\ \frac{1}{8} & \frac{1}{8} & \frac{1}{8} & \frac{1}{8} \end{bmatrix} \quad (25)$$

Doing all the computations the inverse of Y(s) is:

$$Y_{8 \times 8}(s)^{-1} = \frac{adj(Y(s))}{\det(Y(s))} = \begin{bmatrix} -1 & \cdots & 0 & 1 \\ \vdots & \ddots & \vdots & \vdots \\ 0 & \cdots & -1 & 1 \\ 1 & \cdots & 1 & 1 \end{bmatrix} \quad (26)$$

As the final step the normalized time shifts (d_i) are calculated from the new set of variables (x_i):

$$\begin{bmatrix} \widehat{d_1} \\ \widehat{d_2} \\ \vdots \\ \widehat{d_8} \end{bmatrix} = Y(s)^{-1} \cdot \begin{bmatrix} \widehat{x_1} \\ \widehat{x_2} \\ \vdots \\ \widehat{x_8} \end{bmatrix} = \begin{bmatrix} -1 & \cdots & 0 & 1 \\ \vdots & \ddots & \vdots & \vdots \\ 0 & \cdots & -1 & 1 \\ 1 & \cdots & 1 & 1 \end{bmatrix} \cdot \begin{bmatrix} \widehat{x_1} \\ \widehat{x_2} \\ \vdots \\ \widehat{x_8} \end{bmatrix} =$$

$$= \begin{bmatrix} \widehat{x_8} - \widehat{x_1} \\ \vdots \\ \widehat{x_8} - \widehat{x_7} \\ \widehat{x_1} + \widehat{x_2} + \cdots + \widehat{x_8} \end{bmatrix} \quad (27)$$

Based on (27) for an 8 module system the decoupled control can be designed as seen in Fig. 5, where d_1 will become $x_8 - x_1$, d_2 will be $x_8 - x_2$ and so on; and $d_8 = x_1 + x_2 + \ldots + x_8$. The results obtained in our Simulink circuit model of the system validates both this control method, the mathematical model of the DAB converter and the PETT for the novel MVDC-RES.
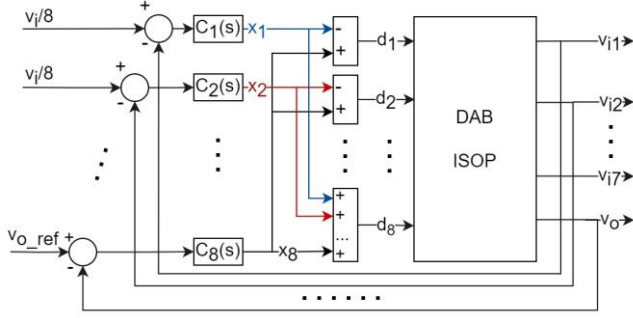
Fig. 5. Control scheme for a four modules system.

4. SIMULATION MODEL

The MVDC PETT designed is an 8-module system capable of 1.2MW of total power, with 25 kV input voltage (3125V input voltage on each module), 1500V output voltage and 10 kHz switching frequency. Fig. 7 presents the whole system with the decoupled control loops on the left and the PETT on the right.
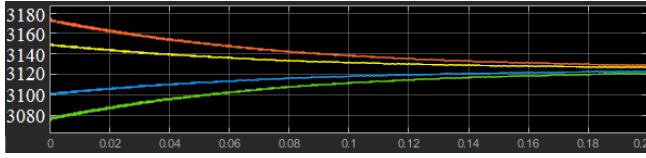

Fig. 6. Different module input voltages balancing out.

Figure 6 illustrates how the input voltages of modules balances out in an ISOP controlled system.

Compensators C_1-C_8 are simple PI controllers, since the transfer function of the system is first order. Fig. 8 represents the leakage inductor current and voltage and the primary voltage. As it can be noticed, I_L and V_L have the same form as in Fig. 1 from 2. On Fig. 9 the output voltage and current is shown.
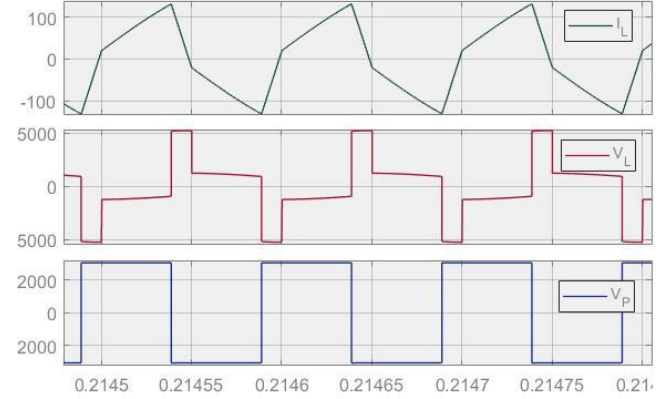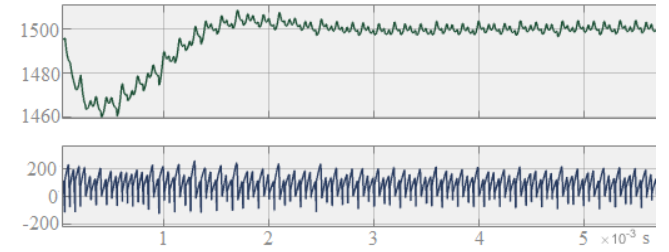

Fig. 8. Primary waveforms.

Fig. 9. Output voltage and current.

Fig. 7. The 8 module PETT system with decoupled control.

The output of the system reaches stability in less than 5 milliseconds and the output voltage ripple is negligible. Fig. 10 shows a closer look of the secondary waveforms. The total harmonic distortion (THD) of the output waveforms are less than 2% in steady state, as seen in Fig. 11.
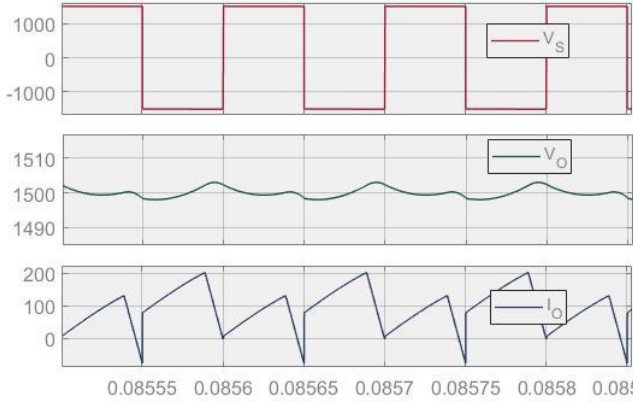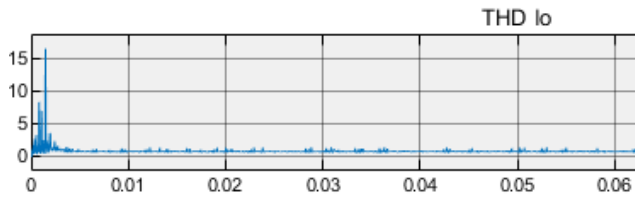

Fig. 10. THD.

Fig. 11. THD.

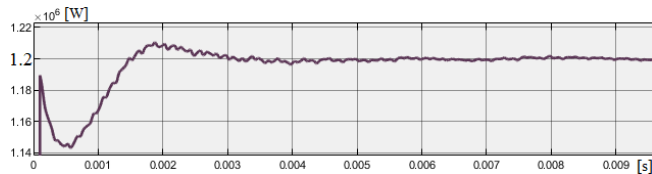Finally, the total output power of 1.2MW can be seen on Fig. 12 below.

Fig. 12. Total output power.

5. CONCLUSIONS

As a conclusion, the paper presented a detailed mathematical deduction of the DAB converter's average model and its connection in ISOP, showing that the electrical quantities of the converters and the control signals are interdependent. In case of identical converter modules, if the possible component mismatches are insignificant, the same control loop with a PI regulator is sufficient, however separate decoupled control loops can improve the input voltage balance. Section 3 presents in detail such a decoupling method of the interdependent variables. Finally in section 4 the full PETT system for the novel MVDC RES is presented with the waveform and THD results. The system is extended with a traction inverter and motor and will be disseminated in a following paper.

REFERENCES

[1] M. Brenna, F. Foiadelli, and D. Zaninelli, *Electrical railway transportation systems*. Wiley, 2018.

[2] I. Ferencz, D. Petreus, and P. Tricoli, "Converter Topologies for MVDC Traction Transformers," *2020 IEEE 26th Int. Symp. Des. Technol. Electron. Packag.*, pp. 362–367, 2020, doi: 10.1109/siitme50350.2020.9292214.

[3] R. Giri, V. Choudhary, R. Ayyanar, and N. Mohan, "Common-duty-ratio control of input-series connected modular DC-DC converters with active input voltage and load-current sharing," *IEEE Trans. Ind. Appl.*, vol. 42, no. 4, pp. 1101–1111, 2006, doi: 10.1109/TIA.2006.876064.

[4] P. Zumel, L. Ortega, A. Lazaro, C. Fernandez, and A. Barrado, "Control strategy for modular dual active bridge input series output parallel," *2013 IEEE 14th Work. Control Model. Power Electron. COMPEL 2013*, 2013, doi: 10.1109/COMPEL.2013.6626418.

[5] A. R. Alonso, J. Sebastian, D. G. Lamar, M. M. Hernando, and A. Vazquez, "An overall study of a Dual Active Bridge for bidirectional DC/DC conversion," *2010 IEEE Energy Convers. Congr. Expo. ECCE 2010 - Proc.*, pp. 1129–1135, 2010, doi: 10.1109/ECCE.2010.5617847.

[6] K. George, "Design and Control of a Bidirectional Dual Active Bridge DC-DC Converter to Interface Solar, Battery Storage, and Grid-Tied Inverters," *Univ. Arkansas, thesis*, 2015.

[7] P. Zumel *et al.*, "Analysis and modeling of a modular ISOP Full Bridge based converter with input filter," *Conf. Proc. - IEEE Appl. Power Electron. Conf. Expo. - APEC*, vol. 2016-May, pp. 2545–2552, 2016, doi: 10.1109/APEC.2016.7468223.